Realization of Low-Voltage Modified CBTA and Design of Cascadable Current-Mode All-Pass Filter

Umut Engin AYTEN[1], *Mehmet SAGBAS*[2], *Shahram MINAEI*[3]

[1] Dept. of Electronics and Comm. Engineering, Yildiz Technical University, Esenler, 34222, Istanbul, Turkey
[2] Dept. of Electric-Electronics Engineering, Yeni Yuzyil University, Zeytinburnu, 34010, Istanbul, Turkey
[3] Dept. of Electronics and Communications Engineering, Dogus University, Acibadem, Kadikoy, 34722, Istanbul, Turkey

ayten@yildiz.edu.tr, sagbasm@gmail.com, sminaei@dogus.edu.tr

Abstract. *In this paper, a low voltage modified current backward transconductance amplifier (MCBTA) and a novel first-order current-mode (CM) all-pass filter are presented. The MCBTA can operate with ±0.9 V supply voltage and the total power consumption of MCBTA is 1.27 mW. The presented all-pass filter employs single MCBTA, a grounded resistor and a grounded capacitor. The circuit possesses low input and high output impedances which make it ideal for current-mode systems. The presented all-pass filter circuit can be made electronically tunable due to the bias current of the MCBTA. Non-ideal study along with simulation results are given for validation purpose. Further, an nth-order cascadable all-pass filter is also presented. It uses n MCBTAs, n grounded resistors and n grounded capacitors. The performance of the proposed circuits is demonstrated by using PSPICE simulations based on the 0.18 μm TSMC level-7 CMOS technology parameters.*

Keywords

Modified current backward transconductance amplifier (MCBTA), current-mode circuits, all-pass filter, active networks.

1. Introduction

All-pass filters (APF) are widely used in analog signal processing in order to shift the phase while keeping the amplitude constant, to produce various types of filter characteristics, and to implement high-*Q* frequency selective circuits. Therefore, numerous circuits are proposed in the literature for realizing all-pass filters (see [1-11] and the references cited therein). However most of these circuits suffer from the use of excessive number of active components. Since power consumption is one of the most important parameters for the circuit designers, they look for simple structures employing no more than one active element. Use of large number of passive components, lack of electronic tunability, use of floating capacitors, and unsuit ability for cascade connection are some of the other disadvantages which we may encounter in previously reported all-pass filters. The proposed circuits in references [1-6] operate in voltage-mode (VM). In addition, the circuit in ref. [7] operates in transadmittance-mode (TAM) where the input is voltage, the output is current. However, the CM based filters where both input and outputs are current [8-16] have been considered favorable owing to properties such as design simplicity, greater linearity, wider dynamic range, higher usable gain, and low power consumption compared with their VM counterparts.

Active circuits and other signal processing circuits play an important role in electronics. One of the versatile components for such applications is current backward transconductance amplifier (CBTA) proposed in 2010 [17]. As a consequence by using CBTA, grounded and floating inductance simulators [18], [19], frequency dependent negative resistor (FDNR) [19], and voltage- and current-mode filters [7], [17], [20-22], oscillators [23], [24], mutually coupled circuit [25] and multiphase sinusoidal oscillator [26] are presented in the literature.

In this paper, firstly, a low-voltage low-power modified CBTA (MCBTA) is proposed and discussed. Then, a new CM APF filter is proposed. The proposed APF employs one grounded capacitor, one grounded resistor and one MCBTA. It has low input current and high output impedance properties which make it ideal for cascade connection. The proposed CM APF is compared with some other previously reported ones as shown in Tab. 1. Although, the filters in [13] and [14] employ less passive component than the proposed filter, they use an active component namely; the z-copy current differencing transconductance amplifier (ZC-CDTA) which has more terminal than the MCBTA. In fact the implementation of the ZC-CDTA needs more transistors than MCBTA which consequently brings more power consumption and larger chip area. Further, a new current-mode general *n*th-order cascadable all-pass filter by cascading *n* first order all-pass section is proposed. It employs *n* grounded capacitors, *n* grounded resistors, and *n* active components. Finally, the simulation results are given for verifying the theoretical analysis.

Ref.	# of Active Components	# of Passive Components	Electronic Tunability	Low Input Impedance	High Output Impedance	Grounded Capacitor	Without matching condition	Mode of Operation
[8]	4	0	yes	yes	yes	-	no	CM
[9]	1*	4	no	no	no	yes	no	CM
[10]	2	1	yes	no	yes	no	yes	CM
[11]	2	1	yes	yes	yes	yes	yes	CM
[12]	1	2	no	no	yes	yes	yes	CM
[13]	1	1	yes	yes	yes	yes	yes	CM
[14]	1	1	yes	yes	yes	yes	yes	CM
[15]	2	1	yes	yes	yes	yes	yes	CM
[16]	2	1	yes	yes	yes	yes	yes	CM
Proposed	1	2	yes	yes	yes	yes	yes	CM

Tab. 1. Comparison of the CM APFs.

* Composed of two NMOS transistors

2. Modified Current Backward Transconductance Amplifier and Circuit Description

A recent publication introduced the concept and implementation of a circuit building block termed CBTA [17]. CBTA is proven useful in many voltage-mode and current-mode analog signal processing applications, such as current-mode and voltage-mode filters, and immittance function simulators; see for example [7], [17-26]. The MCBTA is obtained by modifying the CBTA active component that introduced in [17]. The symbol of the MCBTA and its equivalent circuit are shown in Fig. 1, where p and n are input terminals, w, and z are output terminals. In comparison to the CBTA, the MCBTA differs in the relationship between currents I_w and I_p. While in CBTA $I_p = I_w$ (ideally), for the MCBTA we define $I_p = -I_w$. This will simplify the internal CMOS structure of the MCBTA in comparison to CBTA. The MCBTA terminal equations can be defined as

$$I_z = I_{zc} = g_m(s)(V_p - V_n),\ V_w = \mu_w(s)V_z,$$
$$I_p = -\alpha_p(s)I_w,\ I_n = -\alpha_n(s)I_w. \quad (1)$$

The parameters $\alpha_p(s)$, $\alpha_n(s)$, $\mu_w(s)$ and $g_m(s)$ in (1) are the current, voltage or transconductance gains between the respective terminals. They can be expressed as; $\alpha_p(s) = \omega_{\alpha p}(1 - \varepsilon_{\alpha p})/(s + \omega_{\alpha p})$, $\alpha_n(s) = \omega_{\alpha n}(1 - \varepsilon_{\alpha n})/(s + \omega_{\alpha n})$, $\mu_w(s) = \omega_\mu(1 - \varepsilon_w)/(s + \omega_\mu)$, $g_m(s) = g_o\omega_{gm}(1 - \varepsilon_{gm})/(s + \omega_{gm})$ where $|\varepsilon_{\alpha p}|$, $|\varepsilon_{\alpha n}|$, $|\varepsilon_{gm}|$ known as tracking errors are ideally equal to zero, g_o is the DC transconductance gain. Also $\omega_{\alpha p}$, $\omega_{\alpha n}$, ω_{gm}, ω_μ denote corner frequencies. Note that, in the ideal case, the voltage and current gains ($\mu_w(s)$, $\alpha_p(s)$, $\alpha_n(s)$) are equal to unity.

The number of z-output terminals of the MCBTA can be increased easily by extending current mirrors used in its internal structure. In this case, the currents of the copied z terminals are defined as $I_{zc} = g_m(s)(V_p - V_n)$. Meanwhile, the voltage at w terminal is dependent only to the z terminal.

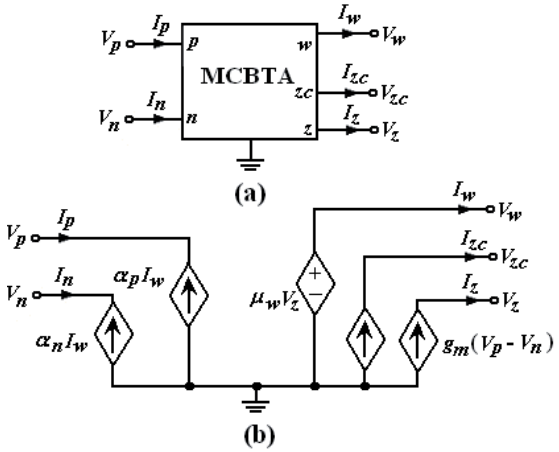

Fig. 1. (a) Block diagram of MCBTA. (b) Equivalent circuit of the MCBTA.

The CMOS implementation of the MCBTA is shown in Fig. 2. It consists of a transconductance stage [27] and a current conveyor stage [28]. The internal circuit of the MCBTA is simpler than CBTA since there is no need to invert the current of the p terminal. Therefore smaller number of transistors is used in the internal structure of the MCBTA than CBTA. The dimensions of the MOS transistors used in the MCBTA implementation are given in Tab. 2. As seen from Fig. 2, the transistors M_{13}–M_{22} are used for realizing a dual-output transconductance stage, while transistors M_2–M_{12} form a current conveyor. In addition the current source I_{REF} and transistor M_1 are employed for biasing purpose. The input voltage is defined as $v_{in} = v_p - v_n$, and i_o is the output current of the transconductance stage. The output current i_o can be found as:

$$i_o = g_m v_{in} = (\sqrt{2I_B K})v_{in} \quad (2)$$

where $K = \mu C_{ox}W_{18,19}/2L_{18,19}$, μ is the mobility of the carrier, C_{ox} is the gate-oxide capacitance per unit area, $W_{18,19}$ is the effective channel width, $L_{18,19}$ is the effective channel length of the transistors M_{18}-M_{19} and I_B is the bias current flowing through M_2.

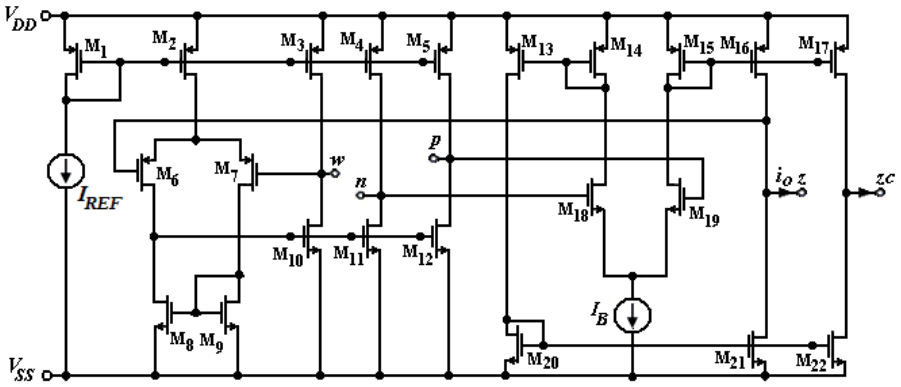

Fig. 2. CMOS implementation of MCBTA.

PMOS Transistors	W(μm)/L(μm)
M_1–M_5	7.2/0.36
M_6, M_7	3.6/0.36
M_{13}–M_{17}	11.52/1.44
NMOS Transistors	W(μm)/L(μm)
M_8, M_9	1.8/0.36
M_{10}–M_{12}	3.6/0.36
M_{18}, M_{19}	4.5/0.36
M_{20}–M_{22}	5.76/1.44

Tab. 2. Dimension of the CMOS transistors.

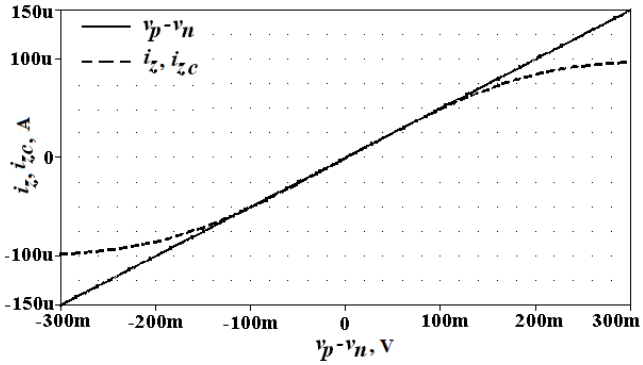

Fig. 3. The transconductance transfer characteristics $i_z = i_{zc} = g_m(v_p - v_n)$.

3. DC and AC Characteristics of the MCBTA

The characteristics of the proposed circuits have been verified using PSPICE simulations. The MCBTAs are simulated using the schematic implementation shown in Fig. 2, with DC power supply voltages equal to $V_{DD} = -V_{SS} = 0.9$ V. I_{REF} and I_B are chosen as 100 μA. The simulations are performed using 0.18 μm level-7 TSMC CMOS technology parameters. Some of the technology parameters used in PSPICE simulations are given as follows: threshold voltage $V_{TH0} = 0.3725$ V, low field mobility $U_0 = 259.53$ cm^2/Vs, and gate oxide thickness $T_{ox} = 4.1.10^{-9}$ m for the NMOS transistor in addition to $V_{TH0} = -0.3948$ V, $U_0 = 109.976$ cm^2/Vs, and $T_{ox} = 4.1.10^{-9}$ m for the PMOS transistor. The power consumption of the MCBTA is 1.27 mW. The DC transconductance transfer characteristics of i_z and i_{zc} against v_p-v_n when $g_m = 0.5$ mS are shown in Fig. 3. For this simulation, a DC voltage sweep between $-0.9\text{ V} \le (v_p - v_n) \le 0.9\text{ V}$ was applied to the p and n terminals of the MCBTA. The output z terminal current was measured while 1 TΩ resistor was connected to the w output of the MCBTA and the output z terminal was grounded. It can be seen that the MCBTA works linearly between $-70\ \mu\text{A} \le i_z \le 70\ \mu\text{A}$ and $-140\text{ mV} \le v_p - v_n \le 140\text{ mV}$ with an error less than 1 %.

The DC characteristic of v_w versus v_z for the proposed MCBTA is obtained as shown in Fig. 4. The DC voltage of the z terminal is sweep between $-0.9\text{ V} \le v_z \le 0.9\text{ V}$ and the output voltage at w terminal was measured while the p and n terminals were grounded. From Fig. 4 it can be seen that the MCBTA works linearly between $-0.75\text{ V} \le v_w \le 0.85\text{ V}$ with an error less than 1 %.

In addition, the DC current transfer characteristics of i_p and i_n terminal currents versus i_w are extracted and shown in Figs. 5a and 5b, respectively. The i_w current was changed between −120 μA and 120 μA and the p and n terminal currents were measured while the z, p and n terminals were grounded. As it can be seen from Fig. 5a and b, the MCBTA works linearly between $-120\ \mu\text{A} \le -i_p \le 105\ \mu\text{A}$ with an error less than 1 %.

In addition, the AC analysis of the CMOS implementation of the MCBTA given in Fig. 2 is investigated. The frequency characteristics, non-ideal parameters (current, voltage and transconductance tracking errors and their corner frequencies) and the maximum operating frequency of the MCBTA are found. The frequency responses of the transconductance gain $|g_m| = |I_z/(V_p - V_n)|$, the voltage gain $|\mu_w| = |V_w/V_z|$, and the current gains $|\alpha_p| = |I_p/I_w|$, $|\alpha_n| = |I_n/I_w|$ are given in Figs. 6 (a-c), respectively. It should be mentioned that the same simulation results are obtained for $|I_p/I_w|$ and $|I_n/I_w|$ both given in Fig. 6c.

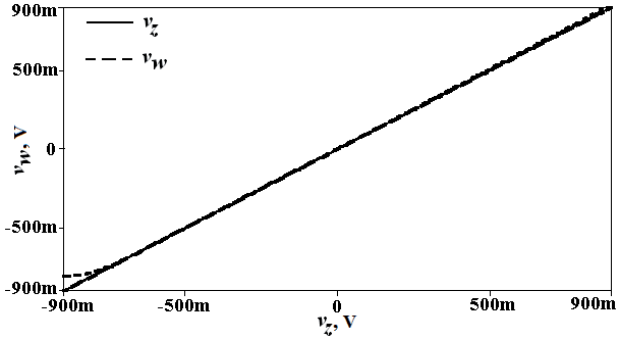

Fig. 4. The voltage transfer characteristic $v_w = v_z$.

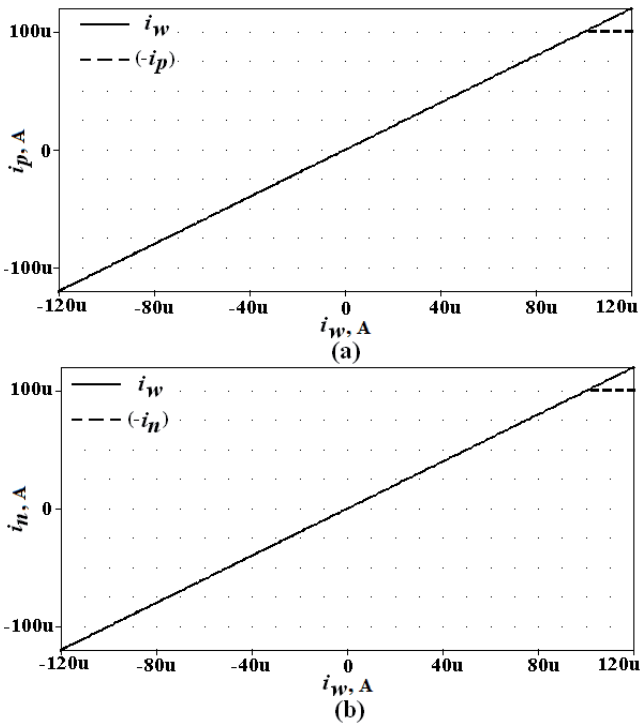

Fig. 5. The current transfer characteristics a) i_p versus i_w, b) i_n versus i_w.

From these simulation results, corner frequencies are found as $\omega_{ap} = 9610$, $\omega_{an} = 9610$, $\omega_{gm} = 650$, $\omega_{\mu} = 9675$ Mrad/s and errors of these gains are $\varepsilon_{ap} = 0.0013$, $\varepsilon_{an} = 0.0013$, $\varepsilon_{gm} = -0.02$ and $\varepsilon_{\mu} = -0.079$, where, g_o is 0.5 mS by choosing $I_B = 100$ µA. As a result, the maximum operating frequency of the MCBTA can be found as follows $f_{\max} = \min\{f_{ap}, f_{an}, f_{gm}, f_{\mu}\} \approx 104$ MHz.

Fig. 7 shows the non-ideal case and high frequency applications device model of the MCBTA, including essential non-idealities such as the high level input and output terminal resistances (R_p, R_n, R_z, R_{zc}), the low level output resistance (R_w) and the input and output capacitances (C_p, C_n; C_z, C_{zc}). This approach is almost acceptable, provided that the implementations of the active devices do not employ multi-stage or complicated parts, which may insert additional poles or zeros to the frequency responses. The parasitic resistances and capacitances values of the MCBTA for proposed CMOS implementation are given in Tab. 3.

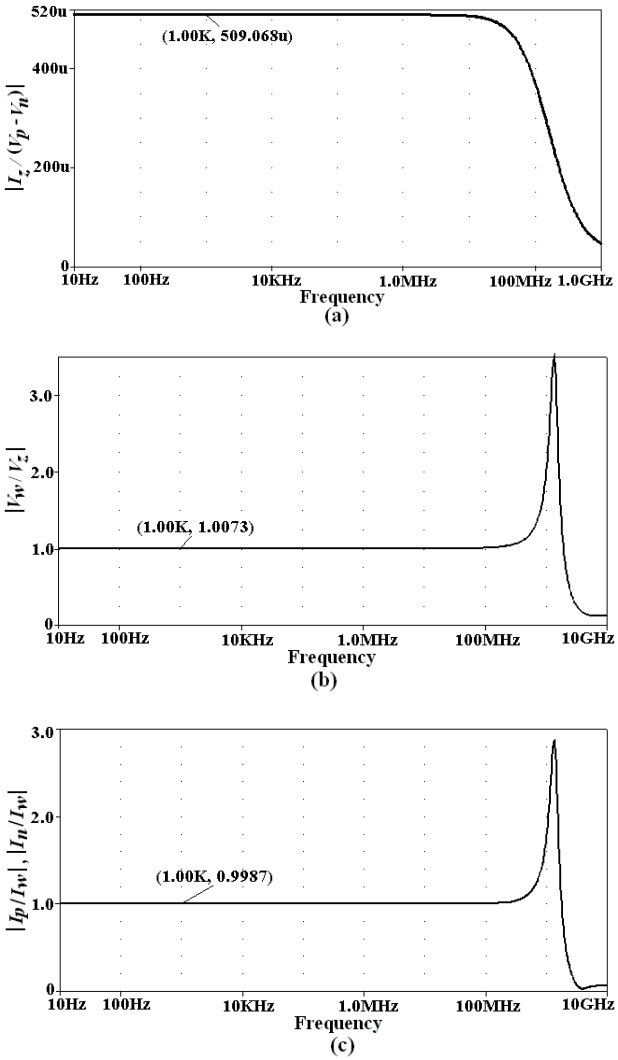

Fig. 6. Frequency responses; a) the transconductance gain, b) voltage gain, c) current gains.

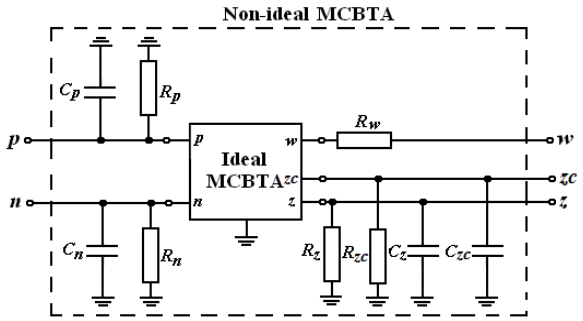

Fig. 7. Parasitic resistance and capacitance of the MCBTA.

Parasitic Impedances	Values
R_p	50.1 kΩ
R_n	50.1 kΩ
R_z	249 kΩ
R_{zc}	249 kΩ
R_w	75 Ω
C_p	180 fF
C_n	180 fF
C_z	244 fF
C_{zc}	196 fF

Tab. 3. Parasitic impedances of the MCBTA.

4. MCBTA Based All-Pass Filter Design

Consider an inverting first-order all-pass (AP) transfer function given by

$$T(s) = \frac{s-\sigma}{s+\sigma}. \tag{3}$$

The proposed current-mode first-order AP filter is shown in Fig. 8. Nodal analysis using (1) yields the following current transfer function

$$T(s) = \frac{I_o(s)}{I_i(s)} = -\frac{sg_mR_1 - g_m/C_1}{s + g_m/C_1}. \tag{4}$$

From (4), the R_1 resistor should be chosen as $g_m = 1/R_1$. Therefore, $\sigma = g_m/C_1$ and the ideal transfer function $T(s)$ has a unity gain and a frequency dependent phase given by

$$T(s) = 2\tan^{-1}(\omega C_1/g_m) \text{ for } g_m = 1/R_1. \tag{5}$$

Fortunately, this matching condition does not affect the AP filter characteristics because it is orthogonally controlled with the external resistor R_1.

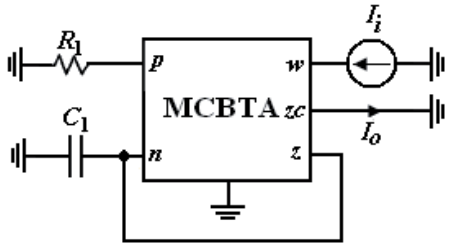

Fig. 8. MCBTA-based current mode first order all-pass filter.

4.1. Effect of Tracking Errors

Fig. 1b shows the equivalent circuit of MCBTA. Here $\alpha_p(s)$, $\alpha_n(s)$ and $\mu_w(s)$ are the current and voltage gains, respectively. $g_m(s)$ is the transconductance gain as defined before.

The effect of the tracking errors can be found from the traditional analysis and by using non-ideal terminal equation of the MCBTA, the current transfer function of the circuit can be written as

$$\frac{I_o(s)}{I_i(s)} = -\frac{s\alpha_p g_m R_1 - \dfrac{\alpha_n g_m}{C_1}}{s + \dfrac{g_m}{C_1}}. \tag{6}$$

Comparing (6) and (4) it can be realized that the pole of the proposed all-pass filter transfer function does not affect from the non-ideality parameters of the MCBTA.

4.2. Effect of Terminal Impedances

Considering the parasitic resistances (R_p, R_n; R_z, R_{zc}, R_w) and capacitances (C_n, C_p; C_z, C_{zc}) shown in Fig. 7, the total impedances at nodes terminals p and n for the circuit of Fig. 8 can be given as follows

$$Z_{R1} = R_1 \| R_p \| (1/sC_p), \tag{7a}$$

$$Z_{C1} = R_n \| R_z \| (1/sC_1) \| (1/sC_n) \| (1/sC_z). \tag{7b}$$

Therefore, the non-ideal the transfer function of the circuit in terms of α_p, α_n, Z_{R1} and Z_{C1} can be given as,

$$T(s) = -\frac{g_m(\alpha_p Z_{R_1} - \alpha_n Z_{C_1}}{g_m Z_{C_1} + 1}. \tag{8}$$

The non-ideal input and output impedances of the proposed filter can be found as follows

$$Z_i = R_w, \; Z_o = R_{zc} \| (1/sC_{zc}). \tag{9}$$

In ideal condition the output has infinitive impedance property since R_{zc} is the high impedance output terminal of the MCBTA and C_{zc} is almost zero (see Tab. 3). Moreover, since R_w of the MCBTA has low value (ideally zero) the proposed circuit enjoys low input impedance property. Therefore the proposed all-pass filter is fully cascadable. Further, the parasitic impedances can be compensated by choosing the external resistor value (R_1) small enough with respect to the terminal resistance (R_p) and the external capacitor value large enough with respect to the terminal capacitances (C_z, C_n).

5. Design of *n*th-order All-Pass Filter

The general all-pass filters have the transfer function

$$T(s) = \frac{I_o(s)}{I_i(s)} = \frac{D(-s)}{D(s)}. \tag{10}$$

Equation (10) can be rewritten the multiplication of the n all-pass sections as follows

$$T(s) = \prod_{i=1}^{n} \frac{s - s_i}{s + s_i}, \text{ Re } \{s_i\} > 0, \; i = 1,2,\ldots, n \tag{11}$$

where $T(s)$ is the all-pass function defined by the open right half of s-plane poles s_i. If all of the poles/zeros of $T(s)$ are real, it can be realized by cascading n first-order all-pass filter of Fig. 8 with transfer function given in (4). The result is shown in Fig. 9. In this case the transfer function on the obtained nth order all-pass filter is given as

$$T(s) = \prod_{i=1}^{n} \left(-\frac{sg_{mi}R_i - g_{mi}/C_i}{s + g_{mi}/C_i}\right) \tag{12}$$

where $g_{mi} = 1/R_i$ and $s_i = g_{mi}/C_i$, $I = 1, 2, \ldots, n$.

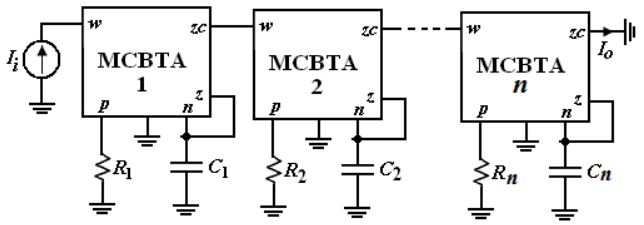

Fig. 9. A general *n*th-order all-pass filter.

6. Design Example and Simulation Results

The fourth-order all-pass filter circuit is realized to verify the performance of the proposed *n*th-order all-pass filter circuit as an example. The proposed fourth-order all-pass filter transfer function is determined to be

$$T(s) = T_1(s)T_2(s) = \left[\frac{s^2 - 2.1s + 1}{s^2 + 2.1s + 1}\right]\left[\frac{s^2 - 2s + 1}{s^2 + 2s + 1}\right] = \left[\frac{s - 0.73}{s + 0.73}\right]\left[\frac{s - 1.37}{s + 1.37}\right]\left[\frac{s - 1}{s + 1}\right]\left[\frac{s - 1}{s + 1}\right]. \quad (13)$$

The passive components values of the 4th-order all-pass filter can be found as follows;

Section I: $C_1 = 1/(0.73R_1\omega_c)$, $g_{m1} = 1/R_1$

Section II: $C_2 = 1/(1.37R_2\omega_c)$, $g_{m2} = 1/R_2$

Section III: $C_3 = 1/(R_3\omega_c)$, $g_{m3} = 1/R_3$

Section IV: $C_4 = 1/(R_4\omega_c,)$ $g_{m4} = 1/R_4$.

The angular frequency is scaled by $\omega_c = 2\pi\times10^6$ rad/s. Firstly, the simulation is done for the first-order all-pass filter circuit shown in Fig. 8. g_m and R_1 are chosen as 0.5 mS and 2 kΩ, respectively and C_1 is found 79.58 pF for $f_c = 1$ MHz. The gain, phase and group delay characteristics of the proposed first-order all-pass filter can be seen in Fig. 10.

To test the input dynamic range of the proposed current-mode first-order all-pass filter, the time-domain simulation of the all-pass filter as an example has been performed for a sinusoidal input signal at $f = 1$ MHz. Fig. 11 shows the time-domain response of the filter where an amplitude of 140 μA (peak to peak) is obtained at the output without significant distortion. The THD value for the current output is less than 0.1% and the total power dissipation of the proposed all-pass filter is found to be 1.27 mW. The famous X–Y pattern (Lissajous pattern) for the circuit as -90° phase shifter is shown in Fig. 13. Since the amplitudes of the input and output of the proposed APF are different, the shape of the simulated phase characteristic in Fig. 12 looks like ellipsis.

The 4th-order all-pass filter circuit using the MCBTA is shown in Fig. 13. This circuit is obtained by cascading four all-pass filter circuits shown in Fig. 8.

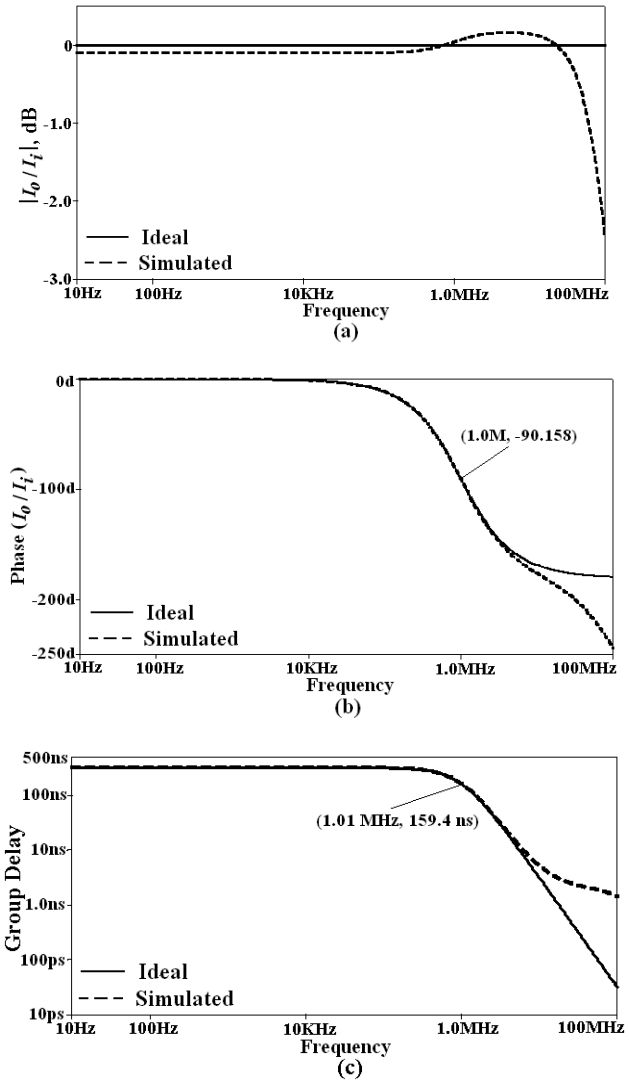

Fig. 10. a) Gain, b) Phase, c) Group delay characteristics of the proposed first-order all-pass filter.

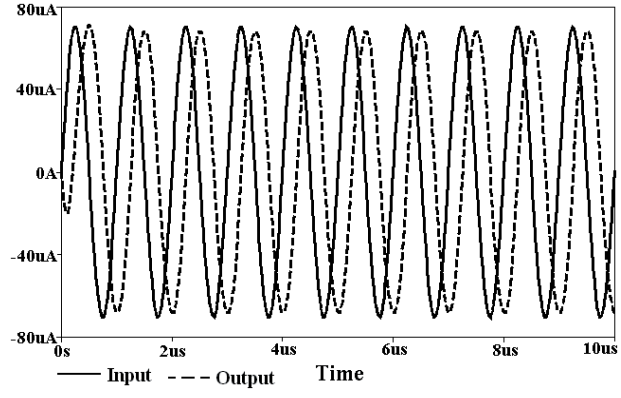

Fig. 11. The input and output waveforms of the proposed first-order all-pass filter.

The proposed 4th-order all-pass filter circuit is built with $R_1 = R_2 = R_3 = R_4 = 1/g_m = 2$ kΩ, $g_m = 0.5$ mS, and $C_1 = 109$ pF, $C_2 = 58$ pF, $C_3 = C_4 = 79.6$ pF for $f_c = 1$ MHz. The simulation results with respect to ideal ones are shown in Fig. 14. It can be seen that the simulated and theoretical

magnitude and phase responses of the all-pass filter are in good agreement

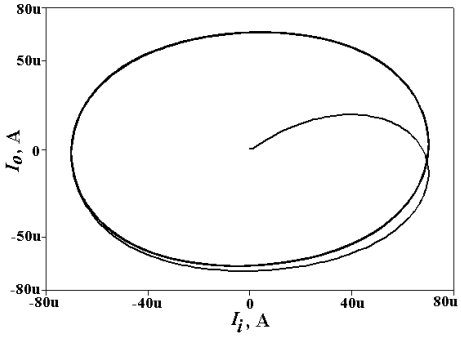

Fig. 12. Lissajous pattern (I_o against I_{in}) for the proposed AP filter.

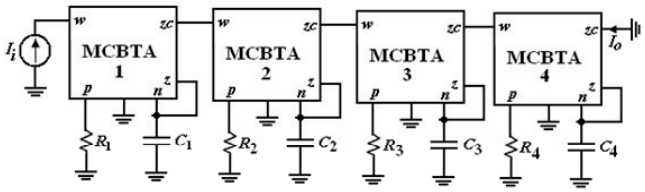

Fig. 13. 4th-order all-pass filter circuit.

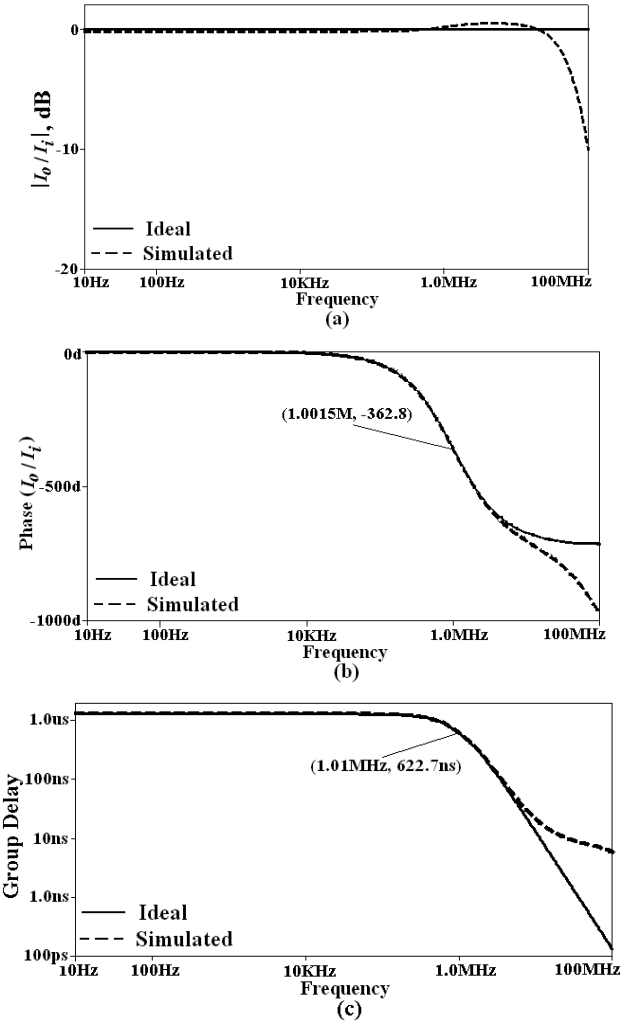

Fig. 14. a) Gain, b) Phase, c) Group delay characteristics of the proposed 4th-order all-pass filter circuit.

From simulation, the gain values of the proposed circuit are 0.98 for frequencies lower than 500 kHz and 1.0152 for the corner frequency 1 MHz, while the theoretical value is one. The phases are measured to be -0.7° at low frequencies and -362° at 1 MHz while they are 0° and 360° respectively for ideal case.

A sinusoidal input current with 70 μA peak value is applied to the circuit and the output signal is observed as shown in Fig. 15a. The simulation results are found in very good agreement with the ideal ones. The FFT spectrum of the input and output signals are shown in Fig. 15b. The THD value for the current output is 2.52% and the total power dissipation of the proposed 4th-order all-pass filter circuit is found to be 5.08 mW.

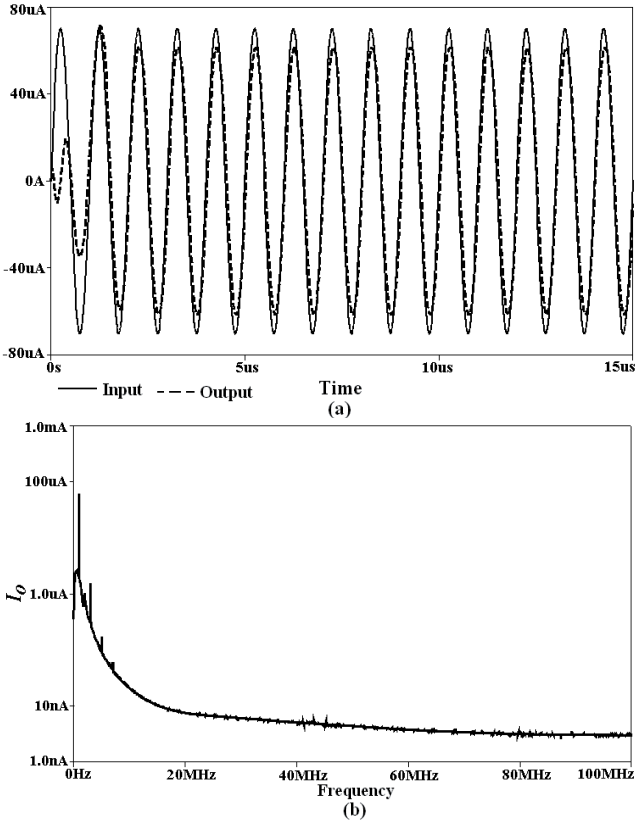

Fig. 15. a) The input and output waveforms of the proposed 4th-order all-pass filter circuit, b) FFT spectrum of the current output.

7. Conclusion

A novel low-voltage low-power MCBTA is proposed and verified through PSPICE simulation using 0.18 μm TSMC level-7 CMOS technology parameters. The MCBTA operates at a low supply voltage of only ±0.9 V and a total power consumption of only 1.27 mW. A novel first-order current-mode all-pass filter using two grounded passive component and one MCBTA is also proposed. The proposed circuit has the advantage of having low input and high output impedances which makes it for easy cascadability. Further, a *n*th-order all-pass filter topology which

uses n MCBTAs, n grounded resistors and n grounded capacitors, is also proposed. As an example, a fourth-order all-pass filter which has only real poles/zeros and low Q value is designed. Non-ideal study along with simulation results are given to verify the theory.

References

[1] MAHESHWARI, S. High input impedance voltage-mode first-order all-pass sections. *International Journal of Circuit Theory and Applications,* 2008, vol. 36, p. 511–512.

[2] CHANG, C. M., SOLIMAN, A. M., SWAMY, M. N. S. Analytical synthesis of low sensitivity high-order voltage-mode DDCC and FDCCII-grounded R and C all-pass filter structures. *IEEE Transactions Circuits and Systems I-Regular Papers*, 2007, vol. 54, p. 1430–1443.

[3] BIOLEK, D., BIOLKOVA, V. All-pass filters employing differential op amps. *Electronics World*, 2010, vol. 116, no. 1891, p. 44 – 45.

[4] METIN, B., PAL, K. Cascadable allpass filter with a single DO-CCII and a grounded capacitor. *Analog Integrated Circuits and Signal Processing*, 2009, vol. 61, no. 3, p. 259–263.

[5] HERENCSAR, N., KOTON, J., JERABEK, J., VRBA, K., CICEKOGLU, O. Voltage-mode all-pass filters using universal voltage conveyor and MOSFET-based electronic resistors. *Radioengineering*, 2011, vol. 20, no. 1, p. 10–18.

[6] MINAEI, S., YUCE, E. Novel voltage-mode all-pass filter based on using DVCCs. *Circuits, Systems, and Signal Processing,* 2010, vol. 29, p. 391–402.

[7] HERENCSAR, N., LAHIRI, A., KOTON, J., SAGBAS, M., AYTEN, U. E. VRBA, K. New MOS-C realization of transadmittance type all-pass filter using modified CBTA. In *Proceeding of International Conference on Applied Electronics (AE 2011)*. Pilsen (Czech Republic), 2011, p. 153 - 156.

[8] MINAEI, S., CICEKOGLU, O. New current-mode integrator and all-pass section without external passive elements and their applications to design a dual-mode quadrature oscillator. *Frequenz*, 2003, vol. 57, no. 1-2, p. 19-24.

[9] YUCE, E., MINAEI, S., HERENCSAR, N., KOTON, J. Realization of first-order current-mode filters with low number of MOS transistors. *Journal of Circuits, Systems, and Computers*, 2013, vol. 22, no. 1, 1250071 14 p.

[10] TANGSRIRAT W., PUKKALANUN, T., SURAKAMPON-TORN, W. Resistorless realization of current-mode first-order allpass filter using current differencing transconductance amplifiers. *Microelectronics Journal*, 2010, vol. 41, p. 178–183.

[11] JAIKLA, W., NOPPAKARN, A., LAWANWISUT, S. New gain controllable resistor-less current-mode first order allpass filter and its application. *Radioengineering*, 2012, vol. 21, no. 1, p. 312-316.

[12] MAHESHWARI, S. High output impedance current-mode all-pass sections with two grounded passive components. *IET Circuits Devices and Systems,* 2008, vol. 2, no. 2, p. 234–242.

[13] LAHIRI, A., CHOWDHURY, A. A novel first-order current-mode all-pass filter using CDTA. *Radioengineering,* 2009, vol. 18, no. 3, p. 300-305.

[14] PANDEY, N., PAUL, S. K. Single CDTA-based current mode all-pass filter and its applications. *Journal of Electrical and Computer Engineering,* 2011, vol. 2011, Article ID 897631.

[15] TANGSRIRAT, W. Cascadable current-mode first-order allpass filter using current controlled conveyors. *Przegląd Elektrotechniczny,* 2013, vol. 89, no. 1a, p. 187-190.

[16] SAFARI, L., MINAEI, S., YUCE, E. CMOS first-order current-mode all-pass filter with electronic tuning capability and its applications. *Journal of Circuits, Systems, and Computers,* 2013, vol. 22, no. 3, 1350007 17 p.

[17] AYTEN, U. E., SAGBAS, M., SEDEF, H. Current-mode leapfrog ladder filter using a new active component. *AEU-International Journal of Electronics and Communications,* 2010, vol. 64, no. 6, p. 503-511.

[18] SAGBAS, M. Component reduced floating ±L, ±C and ±R simulators with grounded passive components. *AEU-Int. Journal of Electronics and Communications,* 2011, vol. 65, p. 794-798.

[19] AYTEN, U. E., SAGBAS, M., HERENCSAR, N., KOTON, J. Novel floating general element simulators using CBTA. *Radioengineering,* 2012, vol. 21, no. 1, p. 11-19.

[20] SAGBAS, M., AYTEN, U. E., SEDEF, H. Current and voltage transfer function filters using a single active device. *IET Circuits Devices and Systems,* 2010, vol. 4, no. 1, p. 78-86.

[21] KOKSAL, M. Realization of a general all-pole current ratio transfer function by using CBTA. *International Journal of Circuit Theory and Applications,* 2013, vol. 41, no. 3, p. 319-329.

[22] SAGBAS, M., KOKSAL, M. Realization of a general resistorless active biquad by using CBTA. *Journal of Circuits, Systems and Computers,* 2012, vol. 21, no. 1, 1250013p.

[23] HERENCSAR, N., KOTON, J., VRBA, K., LAHIRI, A., AYTEN, U. E., SAGBAS, M. A new compact CMOS realization of sinusoidal oscillator using a single modified CBTA. In *Proceeding of 21st International Conference Radioelektronika*. Brno (Czech Republic), 2011, p. 41 - 44.

[24] AYTEN, U. E., SAGBAS; M., SEDEF, H. Electronically tunable sinusoidal oscillator circuit with current and voltage outputs. *Int. Journal of Electronics,* 2012, vol. 99, no. 8, p. 1133-1144.

[25] KOKSAL, M., AYTEN, U. E., SAGBAS, M. Realization of new mutually coupled circuit using CC-CBTAs. *Circuits, Systems, and Signal Processing,* 2012, vol. 31, no. 2, p. 435 - 446.

[26] SAGBAS, M. AYTEN, U. E., HERENCSAR, N., MINAEI S. Voltage-mode multiphase sinusoidal oscillators using CBTAs. In *Proceedings of the 2012 35th International Conference on Telecommunications and Signal Processing (TSP 2012).* Prague (Czech Republic), 2012, p. 421 - 425.

[27] KAEWDANG, K., SURAKAMPONTORN, W. On the realization of electronically current-tunable CMOS OTA. *AEU-International Journal of Electronics and Communications,* 2007, vol. 61, p. 300 to 306.

[28] GUNES, E. O., ZEKI, A., TOKER, A. Design of a high performance mutually coupled circuit. *Analog Integrated Circuits and Signal Processing,* 2011, vol. 66, no. 1, p. 81-91.

About Authors ...

Umut Engin AYTEN received the M.Sc. and Ph.D. degrees in Electronics Engineering from the Yildiz Technical University, Istanbul, Turkey, in 2003 and 2009, respectively. He is currently an Asst. Professor at Yildiz Technical University. His current field of research concerns analog integrated circuits, active filters, current-mode circuits and analog signal processing.

Mehmet SAGBAS received his B.S. degree in Electronics Engineering from the Istanbul Technical University in 2000. He received his M.S. degree in Electronics Engineering from the Fatih University in 2004. He received his Ph.D. degree in Electronics Engineering from the Yildiz Technical University in 2007. He is currently an Assoc. Professor at Yeni Yuzyıl University. His research interests are analog integrated circuits and analog signal processing.

Shahram MINAEI received the B.Sc. degree in Electrical and Electronics Engineering from Iran University of Science and Technology, Tehran, Iran, in 1993 and the M.Sc. and Ph.D. degrees in Electronics and Communication Engineering from the Istanbul Technical University, Istanbul, Turkey, in 1997 and 2001, respectively. He is currently a Professor in the Department of Electronics and Communication Engineering, Dogus University, Istanbul, Turkey. He has more than 140 publications in scientific journals or conference proceedings. His current field of research concerns current-mode circuits and analog signal processing. Dr. Minaei is a senior member of the IEEE, an associate editor of the Journal of Circuits, Systems and Computers (JCSC), and an area editor of the International Journal of Electronics and Communications (AEÜ).